

Inferring Plio-Pleistocene Southern African Biochronology From Facial Affinities in *Parapapio* and Other Fossil Papionins

F.L. Williams,^{1*} R.R. Ackermann,² and S.R. Leigh³

¹Department of Anthropology, Georgia State University, Atlanta, GA

²Department of Archaeology, University of Cape Town, Cape Town, Rondebosch 7701, South Africa

³Department of Anthropology, University of Illinois, Urbana-Champaign, Urbana, IL

KEY WORDS African cercopithecids; *Papio*; *Theropithecus*; *Dinopithecus*; *Australopithecus*

ABSTRACT Buried in the same South African cave deposits as *Australopithecus*, fossil papionins have been referred to *Parapapio* (*Pp. whitei*, *Pp. broomi*, *Pp. jonesi*, *Pp. antiquus*), *Papio* (*P. izodi*, *P. angusticeps*, *P. h. robinsoni*), *Theropithecus* (e.g., *T. darti*), *Gorgopithecus*, or *Dinopithecus* on the basis of postcanine tooth size and descriptive morphology of the muzzle. The morphological patterns of variation that these papionins demonstrate can help to place the *Australopithecus* fossils into a biochronological context and provide valuable information for reconstructing regional Plio-Pleistocene turnover. To document these patterns of variation across fossil-bearing sites, we explore morphometric affinities within *Parapapio*, and between *Parapapio* and other Plio-Pleistocene taxa (*Dinopithecus ingens*, *Papio angusticeps*, *Papio*

izodi, and *Theropithecus darti*) by analyzing a sample of interlandmark distances derived from 3-D coordinate data of the most complete fossil papionin specimens available. Bivariate and multivariate analyses show that *Pp. whitei* exhibits as much variation between sites and between individuals as *Pp. broomi* and *Pp. whitei* combined. Diversity in *Parapapio* at Makapansgat and Sterkfontein may suggest substantial time depth to the caves. *Theropithecus darti*, *Dinopithecus ingens*, *Papio angusticeps*, *Pp. whitei* from Bolt's Farm (BF 43), and *Pp. jonesi* from Sterkfontein (STS 565) differ considerably from one another. Other *Parapapio* specimens across sites form a separate cluster with *P. izodi* from Taung, suggesting a Pliocene age for this site. *Am J Phys Anthropol* 132:163–174, 2007. © 2006 Wiley-Liss, Inc.

Southern African caves provide a rich assemblage of cercopithecoid fossils that preserve some of the earliest morphological evidence for the evolution of extant African papionins. Since these papionins are found in southern African fossil-bearing deposits, they provide important contextual information regarding australopithecoid/early *Homo* paleoecology and biostratigraphic dating (Delson, 1984; McKee, 1993a; Benefit, 1999; El-Zaatari et al., 2005). One genus, *Parapapio*, is particularly well represented at Sterkfontein, Makapansgat, Taung, and to some extent, at Swartkrans, Kromdraai, and Bolt's Farm. Here we explore patterns of variation characterizing *Parapapio* and other Plio-Pleistocene southern African papionins to improve the efficacy of using these taxa as biochronological indicator species within and between South African fossil-bearing sites.

Dating of South African caves

Reconstructing the evolutionary sequence of *Australopithecus* within and between sites is plagued by the extreme intricacy of South African karstic deposits. This complexity derives from multi-stage infilling, irregular deposition, regional uplift, and commercial quarrying that have combined to degrade the stratigraphic integrity of the sites (Brain, 1981; Partridge et al., 2000). Since the caves lack available chronometric dating sequences, most age estimates are based on correlations of first and last appearances of southern African fossil mammals to the chronometrically dated East African fauna (Brain, 1981; Delson, 1984; Vrba, 1996, 2000; Partridge et al., 2000). Weak paleomagnetic signals have

placed Makapansgat and Sterkfontein in the Pliocene (Partridge, 2000; Partridge et al., 2000), while Kromdraai B may straddle the Plio-Pleistocene boundary (Thackeray et al., 2002). The ordinal positions of Swartkrans (Members 1–3), Kromdraai (A and B), Taung and Drimolen are primarily based on faunal correlations between sites (Freedman and Brain, 1972; Brain, 1981; Delson, 1984; McKee, 1993a; McKee et al., 1995; Keyser et al., 2000; Watson, 2004). Table 1 shows a biochronology of fossil southern African papionins modified from Delson's (1984, 1988) African cercopithecoid zones. These zones depict biochrons, or the extent to which a taxon is dispersed over chronometric time. Biochronology is distinct from biostratigraphy, assessment of FADs and LADs, and other approaches to faunal dating because it avoids circularity by ultimately relying on external estimates of time (Delson, 1984). We essentially accept Delson's biochronology for southern African sites as a point

Grant sponsors: LSB Leakey Foundation; Wenner-Gren Foundation for Anthropological Research; National Research Foundation of South Africa; Research Team Grant, Georgia State University.

*Correspondence to: Frank L'Engle Williams, Department of Anthropology, Georgia State University, P.O. Box 3998, Atlanta, GA 30303, USA. E-mail: frankwilliams@gsu.edu

Received 6 October 2005; accepted 8 August 2006

DOI 10.1002/ajpa.20504

Published online 31 October 2006 in Wiley InterScience (www.interscience.wiley.com).

TABLE 1. Biochronology of South African sites

Age (Mya)	A-C zones ¹	South African fossil-bearing sites	Representative species
1.5	6 upper	Gladysvale	<i>P. angusticeps</i>
	6 lower	Kromdraai A	<i>P. angusticeps</i>
	5	Swartkrans Member 1	<i>D. ingens</i>
2.0	4 upper	Bolt's Farm Pit 23	<i>Pp. whitei</i>
	4 lower	Taung	<i>Pp. broomi</i> , <i>Pp. whitei</i> (cf. <i>Pp. antiquus</i>) <i>P. izodi</i> (cf. <i>P. wellsi</i>)
2.5	3 upper	Sterkfontein Member 4	<i>Pp. broomi</i> , <i>Pp. whitei</i> <i>Pp. jonesi</i>
3.0	3 lower	Makapansgat Members 3–4	<i>Pp. broom</i> , <i>Pp. whitei</i> <i>T. darti</i>

¹ A-C (African-cercopithecoid) zones developed by Delson (1984, 1988) are calibrated using East African (e.g., Omo, Turkana, Olduvai, and Hadar) chronometric and magnetostratigraphic dates (as well as paleomagnetic signals from Makapansgat), and correlated to the temporal ranges of cercopithecoid fossil taxa from East and South Africa. The Makapansgat fossils derive from the Upper Phase I breccia, West Quarry, and correspond to Member 3 and the lower portion of Member 4; the Sterkfontein fossils originate from Member 4; the Swartkrans specimens are from Member 1. The approximate chronological order of sites, from oldest to youngest, is Makapansgat Members 3–4, Sterkfontein Member 4, Taung, Bolt's Farm Pit 23, Swartkrans Member 1, Kromdraai A and Gladysvale, following Delson (1984, 1988) and Berger et al. (1993).

of departure. Morphometric data from southern African papionin fossils are then explored to assess the validity of this widely accepted biochronology.

Papionins as biochronological indicators

Researchers have often used southern African fossil papionins as indicators of distinct time intervals (Gear, 1926; Jones, 1937; Broom and Jensen, 1946; Szalay and Delson, 1979; Delson, 1984, 1988, 1992; Vrba, 1994, 1996, 2000; Benefit, 1999). One possible justification for this is sized-based. Assuming the ancestors of papionin primates to be small, and probably similar to the relatively small, generalized *Parapapio* fossils from Africa (Szalay and Delson, 1979; Delson, 1984; Jablonski, 2002), the abundance of this genus with respect to other larger papionin taxa roughly indicates the antiquity of fossil-bearing sites. Williams (2004) found that *Parapapio* consistently predominates at the Pliocene deposits of Makapansgat (Members 3–4), Sterkfontein (Members 2 and 4), and Taung, whereas it is largely absent from the more recent Pleistocene sites of Kromdraai B, Swartkrans (Members 2 and 3), and Drimolen; the exception includes material from Swartkrans Member 1 and Kromdraai A, which has been attributed to *Pp. jonesi* (Freedman, 1957; El-Zaatari, 2005). Meanwhile, fossil *Papio*, fossils *Theropithecus*, *Dinopithecus* and *Gorgopithecus* have primarily been identified at the more recent sites of Kromdraai and Swartkrans, although they may also exist in small numbers at Makapansgat (*T. darti*), Sterkfontein Member 4 (*Papio* sp.), and Taung (*P. izodi* (cf. *P. wellsi*)) (Freedman, 1965).

Given this general pattern, it is also possible that distinct biochronological signals exist within *Parapapio* (Table 1). In particular, if it can be shown that *Parapapio* species are distinct, then it may be possible to further refine the relative time sequence of the sites based on the discontinuity of patterns of variation characterizing taxa within *Parapapio*. Similarly, if patterns of variation exhibited by fossil papionin genera can be distinguished, then these distinct morphologies, when present at multiple sites, may indicate rough biochronological equivalence. Alternatively, if single sites contain discontinuous patterns of variation, then these deposits may record extended time intervals. This assumes that indi-

viduals attributed to the same species within and across sites will cluster together, while genera, with respect to one another, will exhibit discontinuities in morphology.

In addition to morphological patterns, another potential biochronological signal is the degree to which sexual dimorphism is expressed. In *Parapapio*, the differences between males and females are far less distinct than those characterizing modern papionins. Patterns of sexual dimorphism are uniformly easier to ascertain in Pleistocene papionins compared with those of their presumptive Pliocene counterparts. The extreme facial prognathism of large adult males is one way in which sexual dimorphism is expressed in papionins, particularly in Pleistocene *Papio*-like taxa.

Papionin morphology

Fossil papionins have been attributed to numerous genera and species throughout the twentieth century, often with much disagreement among scholars as to which individuals belong to each taxon. The genus *Parapapio* is often distinguished from extant and fossil *Papio* by its shortened muzzle, lack of an ante-orbital drop, a steeply sloping facial angle as viewed from *norma lateralis*, a limited degree of sexual dimorphism, smaller overall cranial size, reduced supraorbital torus development, reduced M₃ hypoconulid, reduced or absent maxillary and mandibular fossae, and lack of sagittal cresting (Gear, 1926; Jones, 1937; Broom and Jensen, 1946; Szalay and Delson, 1979; Delson, 1992; Jablonski, 2002; Leigh et al., 2003). *Parapapio* from South African sites is traditionally divided into four species, *Pp. jonesi*, *Pp. whitei*, *Pp. broomi*, and *Pp. antiquus*, although species attribution within *Parapapio* is equivocal (cf. Gear, 1926; Jones, 1937; Broom and Jensen, 1946; Freedman, 1957, 1961, 1965, 1976; Maier, 1970; Freedman and Stenhouse, 1972; Szalay and Delson, 1979; Jablonski, 2002; Fourie, 2006). *Pp. antiquus* is limited to Taung and may be *Pp. broomi* (Freedman, 1976), or *Pp. whitei*. Species of *Parapapio* have previously been identified on the basis of molar size; *Pp. jonesi* has the smallest and *Pp. whitei* has the largest molars. However, the ranges for most postcanine teeth can be encompassed within *Pp. broomi* (Freedman, 1957; Freedman and Stenhouse, 1972). Several researchers have explored nonmetric craniofacial

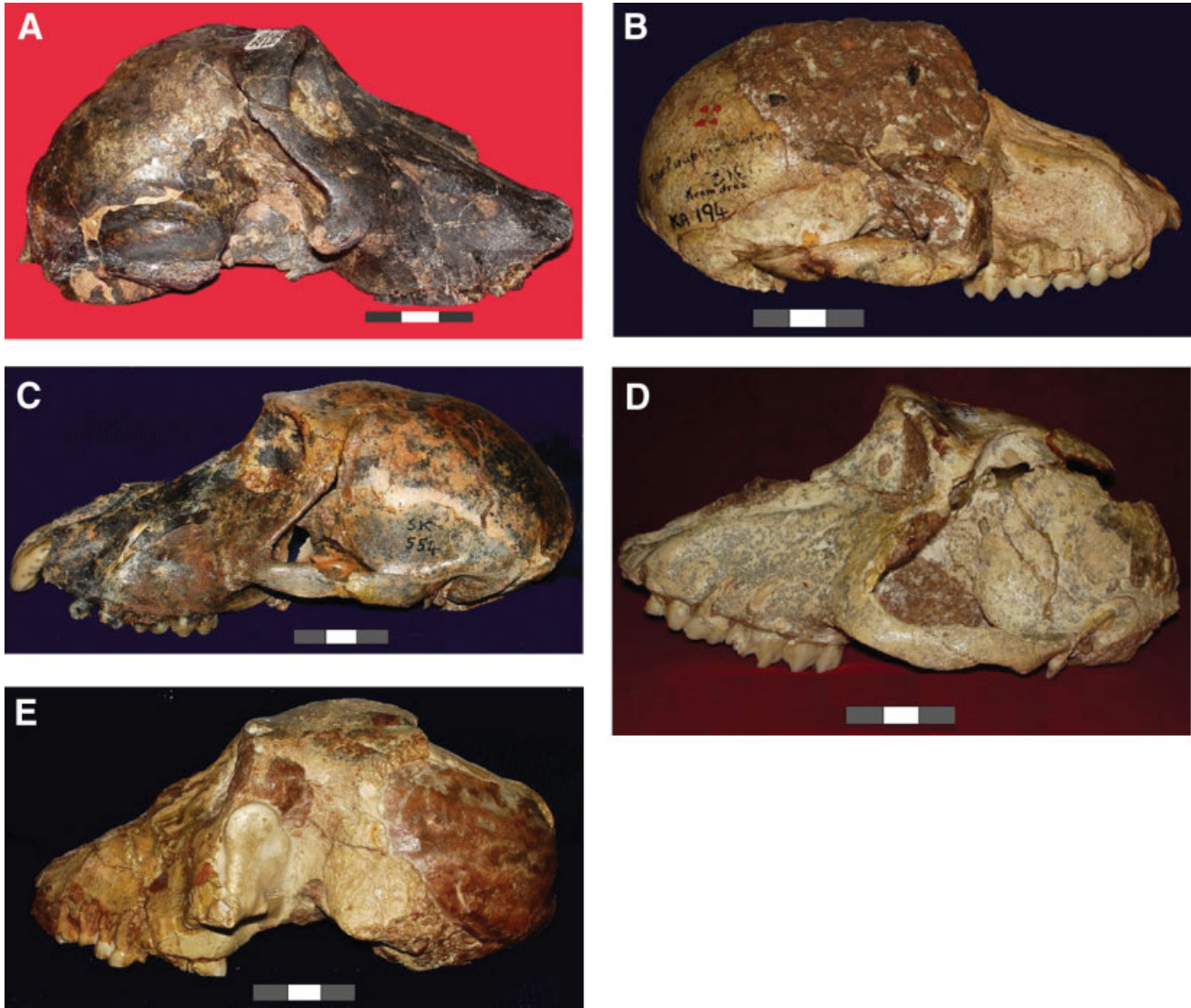


Fig. 1. (a) *Parapapio whitei* (BF 43). This well preserved cranium exhibits a tall snout and pronounced nasal ridges. Although the canine root and accompanying superstructures on the muzzle project laterally and superiorly, no true maxillary fossae are present. The premaxilla is everted anteriorly below the nasal aperture, forming a slightly concave anterior snout. The scale bar is in centimeters. (b) *Papio angusticeps* (KA 194). The type specimen of this taxon exhibits an ante-orbital drop, poorly defined maxillary fossae, and a snout that is broadened posteriorly and narrowed anteriorly. The scale bar is in centimeters. (c) *Dinopithecus ingens* (SK 554). This nearly complete cranium of a juvenile exhibits deciduous molars, permanent central incisors and first molar fully erupted, but the second molar, permanent lateral incisors and canines are unerupted. The snout is elongated and the cranium is superoinferiorly compressed. The scale bar is in centimeters. (d) *Theropithecus darti* (MP 222). This specimen exhibits distinctively tall crests on its molars, a small premaxilla, and curved nasal bones. Heavily accentuated brow ridges converge in the midline of the posterior calvarium. The supratoral sulcus is flat and broad. The scale bar is in centimeters. (e) *Parapapio jonesi* (STS 565). This specimen exhibits slightly concave and shortened nasal bones. The poorly preserved premaxilla narrows from a relatively elongated and posteriorly broadened snout. The scale bar is in centimeters. [Color figure can be viewed in the online issue, which is available at www.interscience.wiley.com.]

morphology as a means for distinguishing between the species of *Parapapio* (Broom and Jensen, 1946; Freedman, 1957, 1960, 1961, 1965, 1976; Maier, 1970; Delson, 1992; Jablonski, 2002).

Papio is normally recognized by a concavity of the nasal bones and a relatively elongated snout (Szalay and Delson, 1979; Jablonski, 2002; Frost et al., 2003). In addition to the larger extant forms (e.g., *Papio hamadryas*), and their extinct Pleistocene relatives (*P. h. robinsoni*), smaller forms of this genus are similar in size to most *Parapapio* specimens, and include *P. izodi* (cf. *P.*

wellsi, Freedman, 1961), *P. angusticeps* (Freedman, 1976; McKee and Keyser, 1994) and extant *P. h. kindae* (Leigh, 2006). Although *P. angusticeps* and *P. izodi* have both been attributed to *Parapapio* by different researchers, they are widely considered *Papio* by recent investigators (Freedman, 1976; Delson, 1992; Jablonski, 2002). While some suggest that all of the small *Papio* specimens from Taung, Kromdraai, Cooper's and Haasgat should be referred to *P. izodi* (Szalay and Delson, 1979; Jablonski, 2002), others, such as McKee and Keyser (1994), refer specimens from Haasgat, Cooper's Cave and

TABLE 2. List of specimens by site, taxon, and developmental stage ($n = 33^{1,2}$)

Specimen	Site	Genus	Species	Life stage	Sex
BF 43	Bolt's Farm	<i>Parapapio</i>	<i>whitei</i>	Adult	Male
GV 4040	Gladysvale	<i>Papio</i>	<i>angusticeps</i>	Adult	Female
KA 194	Kromdraai A	<i>Papio</i>	<i>angusticeps</i>	Adult	Female?
MP 118	Makapansgat	<i>Parapapio</i>	<i>broomi</i>	Juvenile	Unknown
MP 166	Makapansgat	<i>Parapapio</i>	species indet	Juvenile	Unknown
MP 208	Makapansgat	<i>Parapapio</i>	<i>whitei</i>	Subadult	Female
MP 221	Makapansgat	<i>Parapapio</i>	<i>whitei</i>	Adult	Male
MP 222	Makapansgat	<i>Theropithecus</i>	<i>darti</i>	Adult	Unknown
MP 223	Makapansgat	<i>Parapapio</i>	<i>whitei</i>	Adult	Male
MP 224	Makapansgat	<i>Parapapio</i>	<i>broomi</i>	Juvenile	Female
MP 239	Makapansgat	<i>Parapapio</i>	<i>whitei</i>	Adult	Male
MP 3070	Makapansgat	<i>Parapapio</i>	<i>whitei</i>	Adult	Female
MP 3134	Makapansgat	<i>Parapapio</i>	species indet	Juvenile	Unknown
SK 553	Swartkrans	<i>Dinopithecus</i>	<i>ingens</i>	Adult	Male
SK 554	Swartkrans	<i>Dinopithecus</i>	<i>ingens</i>	Juvenile	Female?
STS 373B	Sterkfontein	<i>Parapapio</i>	<i>broomi</i>	Juvenile	Unknown
STS 251	Sterkfontein	<i>Parapapio</i>	<i>broomi</i>	Subadult	Female
STS 254A	Sterkfontein	<i>Parapapio</i>	<i>broomi</i>	Adult	Female
STS 324	Sterkfontein	<i>Parapapio</i>	species indet	Juvenile	Female?
STS 345	Sterkfontein	<i>Parapapio</i>	<i>broomi</i>	Juvenile	Unknown
STS 364	Sterkfontein	<i>Parapapio</i>	species indet	Juvenile	Unknown
STS 368A	Sterkfontein	<i>Parapapio</i>	<i>broomi</i>	Adult	Female
STS 397	Sterkfontein	<i>Parapapio</i>	<i>broomi</i>	Adult	Female
STS 534	Sterkfontein	<i>Parapapio</i>	<i>broomi</i>	Adult	Male
STS 565	Sterkfontein	<i>Parapapio</i>	<i>jonesi</i>	Adult	Female?
SWP 12	Sterkfontein	<i>Parapapio</i>	<i>broomi</i>	Adult	Female
SWP 1733	Sterkfontein	<i>Parapapio</i>	<i>broomi</i>	Juvenile	Unknown
T 17	Taung	<i>Parapapio</i>	<i>broomi</i>	Adult	Female?
T 89-154	Taung	<i>Parapapio</i>	<i>whitei</i>	Adult	Male
TaungNu	Taung	<i>Parapapio</i>	<i>whitei</i>	Adult	Male
TP 10	Taung	<i>Papio</i>	<i>izodi cf. wellsi</i>	Adult	Female
TP 11	Taung	<i>Papio</i>	<i>izodi cf. wellsi</i>	Adult	Unknown
TP 9	Taung	<i>Parapapio</i>	<i>whitei cf. antiquus</i>	Adult	Female

¹ The 15 specimens in bold figured heavily in the multivariate analyses.

² Sex of the specimens may be related to species attribution as indicated in our sample where *Pp. broomi* adults are primarily female, and *Pp. whitei* adults are largely male.

Kromdraai to *P. angusticeps*. The presence of the smaller *P. angusticeps* and larger *P. h. robinsoni* at both Kromdraai and Swartkrans complicates species attributions further. The two forms may also represent males and females of a single polytypic *Papio* species (*P. h. robinsoni*). Alternatively, Cooper's cave has yielded small male *P. angusticeps* (e.g., CO 100, CO 101, CO 135a) that differ considerably from the larger more prognathic *P. h. robinsoni*, and from extant *Papio* (Freedman, 1957; McKee and Keyser, 1994).

Both fossil *Papio* and *Parapapio* can be separated from *Dinopithecus*, *Gorgopithecus* and fossil *Theropithecus* by size and shape of the muzzle, and in most instances, by the absolutely larger teeth in the latter three genera. *Theropithecus* (cf. *Simopithecus*), found at Makapansgat and Swartkrans, is characterized by its distinct molar morphology and relatively reduced anterior teeth. Large cranial superstructures and deep mandibular corpora in this taxon suggest grassland foraging with limited incisal processing of foods (Szalay and Delson, 1979; Jablonski, 2002). *Gorgopithecus* and *Dinopithecus* are large *Papio*-like forms that derive primarily from Kromdraai and Swartkrans, respectively. *Gorgopithecus* may be the largest of southern African papionins and is represented by numerous jaw fragments and one relatively complete but distorted cranium. *Dinopithecus* can be identified by its distinct muzzle morphology which lacks the deep maxillary fossae and steep ante-orbital drop characterizing modern baboons (Freedman, 1957).

Although descriptions of dental and skeletal traits have been used to define these fossil papionin taxa (e.g., Freedman, 1957; Maier, 1970; Eisenhart, 1974; Szalay and Delson, 1979; Jablonski, 2002), morphometric traits have only scarcely been consulted to ascertain patterns of variation within these fossil assemblages. Here we examine these patterns of variation in order to explore whether the distribution of these Plio-Pleistocene fossil primates within and between sites can help to situate the *Australopithecus* fossils in an improved biochronology. Because we depend on the accuracy of current taxonomic assignments for interpreting the results, an additional goal is to compare species attributions with juvenile and adult patterns of variation in order to assess their validity.

MATERIALS AND METHODS

Materials

Our sample comprises 26 individuals from three *Parapapio* species, *Pp. whitei*, *Pp. broomi*, and *Pp. jonesi* as well as seven additional cercopithecoid fossil specimens. The *Parapapio* fossils derive chiefly from Makapansgat and Sterkfontein, although some *Pp. whitei* are from Bolt's Farm (BF 43) and Taung (e.g. TP 9). The number of *Pp. jonesi* specimens is limited, and most of the material attributed to this species is highly fragmentary (Williams, unpublished data). Our *Pp. jonesi* sample consists of STS 565 (Fig. 1), the most complete fossil referred to this species. We also include two Makapans-

gat and two Sterkfontein juvenile *Parapapio* specimens that lack formal species designations. Our dataset includes two individuals that have previously been attributed to *Parapapio antiquus* (e.g., Freedman, 1957; Delson, 1984). We refer one of these (T 17) to *Pp. broomi* and another (TP 9) to *Pp. whitei*. The taxonomy we use is based on museum records and largely corresponds to Freedman (1957, 1976), Szalay and Delson (1979), McKee (1993b) and Jablonski (2002).

These *Parapapio* fossils are compared with specimens referred to *Dinopithecus ingens*, *Papio angusticeps*, *Papio izodi*, and *Theropithecus darti*. *Theropithecus darti* is represented here by a single specimen from Makapansgat (MP 222). The *Dinopithecus* sample contains one fragmentary *Dinopithecus* adult (SK 553), and the beautifully preserved cranium of SK 554 (Fig. 1). Table 2 lists the specimens used in this study, and Figure 1 shows some of the fossils examined (BF 43, KA 194, SK 554, MP 222, STS 565).

Sex was ascribed, when possible, on the basis of canine size and shape; males were designated by long, dagger-shaped canines while females were identified by their shorter, diamond-shaped canines. The fragmentation or absence of the anterior muzzle in adults compounded the normal difficulties associated with sex determination in fossil taxa. Furthermore, it was often impossible to reliably ascribe the sex of juvenile remains that comprise a large proportion of the southern African fossil primate assemblage. This determination of sex resulted in the attribution of 8 males, 16 females and 9 unknowns (Table 2).

Interlandmark distances

Three-dimensional landmarks were digitized on these Plio-Pleistocene fossils by one of us (S.R.L.) at two institutions in South Africa: the School of Anatomical Sciences at the University of the Witwatersrand Medical School in Johannesburg and the Transvaal Museum (Northern Flagship Institution) in Pretoria. Seventeen three-dimensional cranial landmarks were selected following Leigh et al. (2003) and Leigh (2006) to capture the shape of the palate, snout, and upper face. These traits were chosen to correspond closely to growth fields of the face or to bony extremities of the facial bones or both, and include intradentale superior (1); premaxillary suture at alveolar process, right (2); premaxillary suture at alveolar process, left (3); posterior nasal spine (4); nasale (5); zygomaxillare superior, right (6); zygomaxillare superior, left (7); zygomaxillare inferior, right (8); zygomaxillare inferior, left (9); nasion (10); anterior nasal spine (11); maxillary tuberosity, right (12); maxillary tuberosity, left (13); P⁴/M¹, right (14); P⁴/M¹, left (15); lacrimal-maxilla-frontal junction, right (16); and lacrimal-maxilla-frontal junction, left (17). Although a total of 136 unique linear distances are possible from these 17 landmarks, many are poorly represented on the fossils. Table 3 lists the 11 unique interlandmark distances we chose for further analysis based on the preservation of the material.

Lengths, heights, and breadths were chosen to represent the three-dimensional proportions of the muzzle and upper face. Lengths, such as those capturing the maximum extent of the alveolar process, snout, and palate, contrast with mediolateral breadths of the muzzle, alveolar process, and palate along the sagittal plane. Height dimensions include superoinferior distances

TABLE 3. Interlandmark distances with anatomical descriptions

Trait	Interlandmark distance and anatomical description
1	1–4: Intradentale superior to posterior nasal spine (palatal length)
2	1–5: Intradentale superior to nasale (anterior snout height)
3	2–3: Right premaxilla to left premaxilla (premaxilla breadth)
4	6–7: Right zygomaxillare superior to left zygomaxillare superior (upper maxillary breadth)
5	8–9: right zygomaxillare inferior to left zygomaxillare inferior (lower maxillary breadth)
6	12–13: Right maxillary tuberosity to left maxillary tuberosity (posterior alveolar breadth)
7	14–15: Right P ⁴ /M ¹ to left P ⁴ /M ¹ (mid-alveolar breadth)
8	1–13: Intradentale superior to left maxillary tuberosity (alveolar length)
9	1–11: Intradentale superior to anterior nasal spine (premaxillary height)
10	11–12: Anterior nasal spine to right maxillary tuberosity (snout length)
11	4–6: Posterior nasal spine to right zygomaxillare superior (snout height)

along the muzzle dorsum, premaxilla, and anterior snout. We chose not to scale these data since we wanted to preserve the ontogenetic variation in the nonadults.

Methods

Affinities within *Parapapio*. Twenty-four specimens attributed to *Parapapio* sp. are compared in four bivariate scatter plots. These plots reveal the greatest deviations between *Parapapio* specimens. All of these bivariate comparisons show interlandmark distances of the muzzle (anterior snout length, upper maxillary breadth, posterior alveolar breadth, mid-alveolar breadth) plotted against an approximation of palatal length (intradentale superior to the posterior nasal spine); palatal length is used because it is represented for nearly every individual in the sample. T-tests and Mann-Whitney U tests were used to demonstrate significant differences between *Pp. whitei* and *Pp. broomi* adults for 8 out of 11 interlandmark distances. Analysis of Variance (ANOVA) was used to test whether site location (Makapansgat, Sterkfontein and Taung) could effectively sort *Parapapio* fossils (*Pp. whitei* and *Pp. broomi*) regardless of species designation.

Comparisons across fossil papionins. Four bivariate scatter plots compare all 33 specimens simultaneously using an approximation of palatal length (intradentale superior to the posterior nasal spine) along the *x*-axis of each plot, and the four interlandmark distances that showed the greatest divergence between genera (snout height, premaxillary width, alveolar length, lower maxillary breadth) along the *y*-axis. The *x*-axis is represented by palatal length for these bivariate comparisons because the length of the palate is preserved in more individuals than the other measurements.

To examine multivariate relationships across site, taxon, trait, and ontogeny, we compared 15 of the specimens that exhibited all of the 11 interlandmark distances in 2 analyses: a cluster tree using the average linkage method and principal components analysis. To focus on morphological distances between adults, two young juvenile *Parapapio* were excluded before calculating

TABLE 4. Coefficients of variation (CV) and P values for T-tests and Mann-Whitney U tests in *Pp. whitei* (n = 10) and *Pp. broomi* (n = 4) adults¹

Trait	Interlandmark distance	CV for <i>Pp. whitei</i>	CV for <i>Pp. broomi</i>	P values	
				T-test	Mann-Whitney U test
1	1-4: Palatal length	0.187 (n = 9)	0.066 (n = 4)	0.353	0.537
2	1-5: Anterior snout length	0.150 (n = 8)	0.167 (n = 4)	0.453	0.610
3	2-3: Premaxilla breadth	0.102 (n = 8)	0.077 (n = 2)	0.619	0.602
4	6-7: Upper maxillary breadth	0.092 (n = 9)	1.000 (n = 1)	N/A	N/A
5	8-9: Lower maxillary breadth	0.073 (n = 9)	1.000 (n = 1)	N/A	N/A
6	12-13: Posterior alveolar breadth	0.136 (n = 7)	0.153 (n = 2)	0.632	0.242
7	14-15: Mid-alveolar breadth	0.110 (n = 10)	1.000 (n = 1)	N/A	N/A
8	1-13: Alveolar length	0.153 (n = 6)	0.009 (n = 2)	0.480	1.000
9	1-11: Premaxilla height	0.194 (n = 9)	0.157 (n = 4)	0.715	0.643
10	11-12: Snout length	0.137 (n = 7)	0.034 (n = 3)	0.141	0.425
11	4-6: Snout height	0.184 (n = 9)	0.059 (n = 3)	0.782	0.926

¹ Upper and lower maxillary and mid-alveolar breadths were excluded because of small sample size.

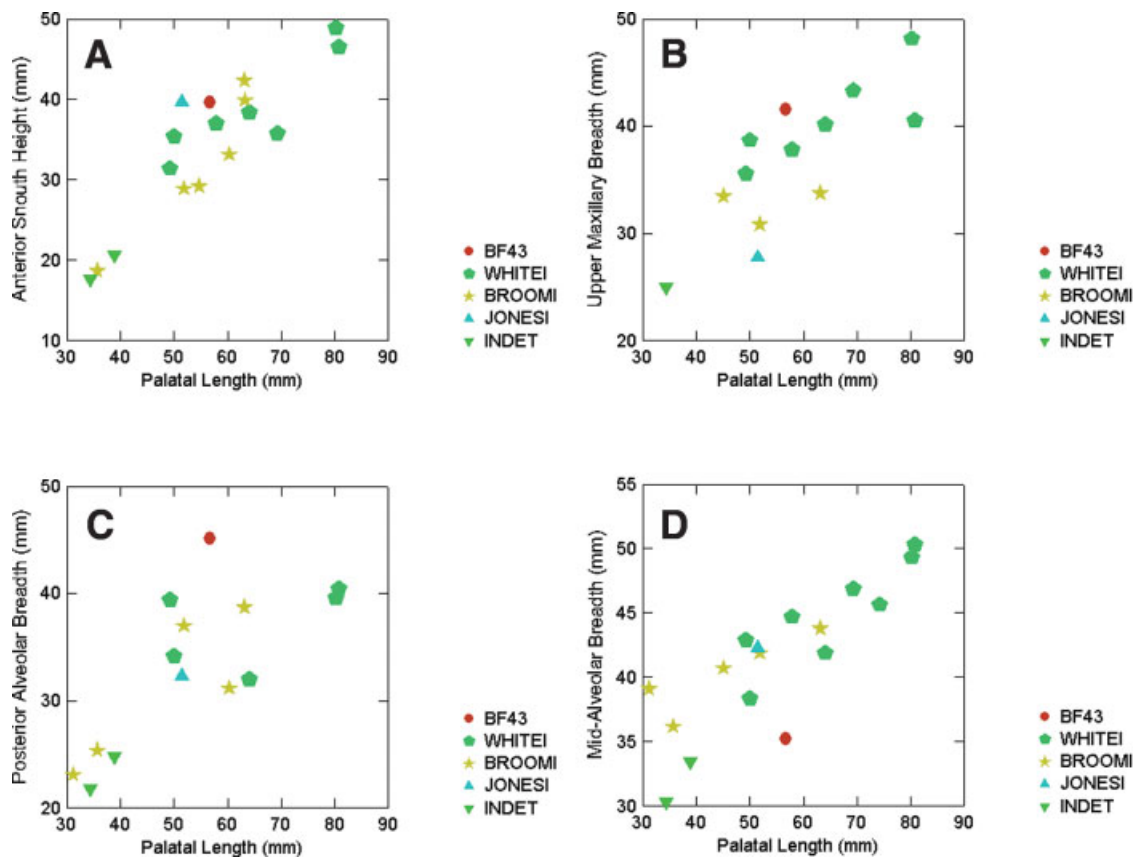


Fig. 2. (a) Anterior snout height compared with palatal length in *Parapapio*. (b) Upper maxillary breadth compared with palatal length in *Parapapio*. (c) Posterior alveolar breadth compared with palatal length in *Parapapio*. (d) Mid-alveolar breadth compared with palatal length in *Parapapio*. [Color figure can be viewed in the online issue, which is available at www.interscience.wiley.com.]

Mahalanobis' distances for 10 variables and 13 individuals; lower maxillary breadth was removed from this test because of its exceptionally large variance.

RESULTS

Affinities within *Parapapio*

Comparisons between adults. When various dimensions of the snout are compared with palatal length, *Pp.*

whitei and *Pp. broomi* broadly overlap. Although coefficients of variation for *Pp. whitei* generally equal or exceed those for *Pp. broomi*, there are also a greater number of *Pp. whitei* adults in our sample compared with the number of adults representing *Pp. broomi* (Table 4). T-tests as well as Mann-Whitney U tests yielded no significant differences between the two for all linear distances available to examine (Table 3).

Two male *Pp. whitei* specimens (MP 221 and MP 223) exhibit particularly long palates compared with other

Parapapio specimens. *Pp. jonesi* (STS 565) differs from other *Parapapio* in its relatively narrow upper maxilla, as do SWP 12, MP 224, and MP 221, albeit to a lesser extent. Despite having a particularly wide posterior alveolar process, BF 43 has a uniquely narrow mid-alveolus given its palate length. STS 254A (*Pp. broomi*) is most similar to BF 43 in its relatively wide posterior alveolar process, but not in mid-alveolar breadth. MP 239 (*Pp. whitei*) and T 17 (*Pp. broomi*) conversely exhibit relatively narrow posterior palates. *Pp. whitei* and *Pp. broomi* specimens generally fall within the same distribution, albeit broadly overlapping, and could be characterized as scaled versions of one another, particularly when the large *Pp. whitei* males, MP 221 and MP 223, are included (Fig. 2). Because the sample included only one adult *Pp. broomi* male, comparisons between the

sexes within and across taxon could not be examined. Most of the juveniles in our sample are attributed to *Pp. broomi*; judging from the placement of individuals within these trajectories, the indeterminate specimens may be *Pp. broomi* as well.

Comparisons between sites. ANOVA was used to determine whether site location (Makapansgat, Sterkfontein, and Taung) could effectively separate traits characterizing *Parapapio* adults attributed to *Pp. whitei* and *Pp. broomi* (i.e., species attribution was ignored). The ANOVA failed to reveal a site-effect on the *Parapapio* fossils (Table 5). The generally low F statistic may suggest a substantial amount of variation within traits. ANOVAs done separately for *Pp. broomi* and *Pp. whitei* (not shown) revealed similar results.

Comparisons across fossil papionins

When all of the fossils are compared as a group, specific taxa and specimens stand apart from the others. For example, *Pp. whitei* from Bolt's Farm, BF 43, can be characterized as exhibiting an extremely tall snout given its palatal length. Meanwhile, *Dinopithecus* extends the pattern observed for other papionin taxa and its juvenile, SK 554, is comparable in size with *Parapapio* adults. *Theropithecus darti*, *P. izodi*, and *P. angusticeps* are broadly similar to the distribution of *Parapapio*, at least in the height of the snout with respect to the length of the palate (Fig. 3a).

When premaxillary width is compared with palate length, *Theropithecus darti*, with its particularly narrow premaxilla, diverges strongly from the other specimens

TABLE 5. ANOVA results for *Parapapio* adults from Makapansgat, Sterkfontein, and Taung

Trait	Interlandmark distance	F	P value
1	1–4: Palatal length	1.764	0.226
2	1–5: Anterior snout length	2.439	0.149
3	2–3: Premaxilla breadth	0.117	0.891
4	6–7: Upper maxillary breadth	2.539	0.159
5	8–9: Lower maxillary breadth	0.982	0.428
6	12–13: Posterior alveolar breadth	0.793	0.502
7	14–15: Mid-alveolar breadth	1.204	0.355
8	1–13: Alveolar length	4.401	0.098
9	1–11: Premaxilla height	1.760	0.226
10	11–12: Snout length	2.875	0.133
11	4–6: Snout height	0.263	0.776

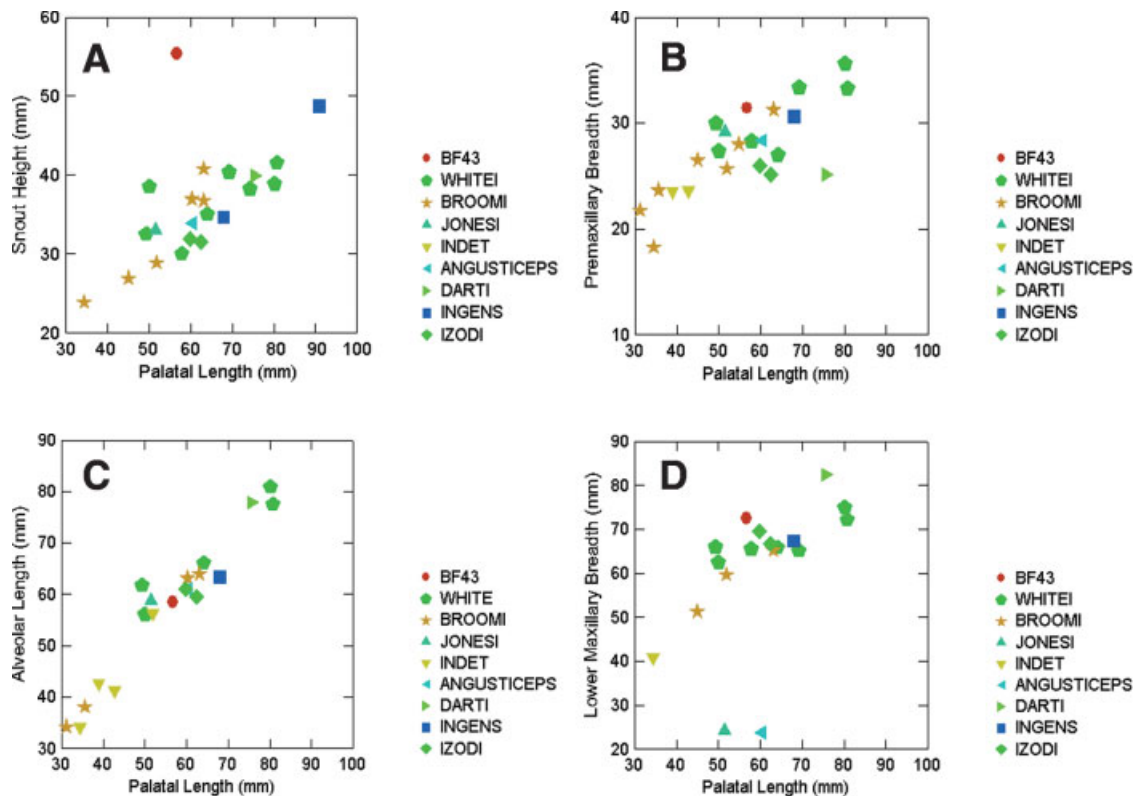


Fig. 3. (a) Snout height compared with palatal length across taxon. (b) Premaxillary breadth compared with palatal length across taxon. (c) Alveolar length compared with palatal length across taxon. (d) Lower maxillary breadth compared with palatal length across taxon. [Color figure can be viewed in the online issue, which is available at www.interscience.wiley.com.]

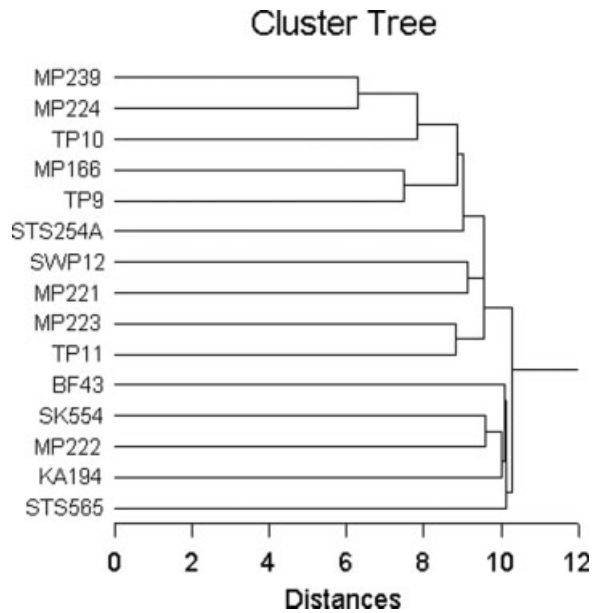


Fig. 4. Cluster analysis of fossil papionins.

(Fig. 3b). Meanwhile, *Dinopithecus ingens*, represented here by the juvenile SK 554 specimen, is larger than most adult *Parapapio* specimens. *Papio izodi* and *P. angusticeps* fall well within the range of *Parapapio* adults, and in this way resemble *Parapapio* more than *Papio*-like *Dinopithecus*. With respect to the premaxilla, Bolt's Farm *Pp. whitei* (BF 43) and *Pp. jonesi* (STS 565) do not differ substantially from other *Parapapio* specimens.

A comparison of alveolar length and palatal length groups two male *Pp. whitei* (MP 221 and MP 223) with *Theropithecus darti* (MP 222). Other *Pp. whitei* specimens are more similar to *Pp. broomi*, *Pp. jonesi* and *P. izodi*. *Dinopithecus ingens* (SK 554) exhibits a relatively large alveolar process with respect to its palate (Fig. 3c). Indeterminate *Parapapio* specimens (MP 166, M 3134, and STS 324) are similar to *Pp. broomi* young juveniles (STS 373B and STS 1733).

When lower maxillary breadth is compared with palatal length across specimens, *Pp. jonesi* (STS 565) and *P. angusticeps* (KA 194) exhibit extremely narrow lower cheek widths given their palatal lengths (Fig. 3d). The relatively pronounced maxillary fossae on both these specimens may help to explain why the lower maxilla narrows medially. Conversely, *Theropithecus darti* (MP 222), and to a lesser extent BF 43, exhibit rather expanded lower snouts that may correspond to strong masticatory stress on the distal molars.

Cluster analysis. A cluster analysis of 15 individuals and 11 traits reveals that *Pp. whitei* and *Pp. broomi* from Makapansgat and Sterktontein, along with *P. izodi* (cf. *P. wellsi*) from Taung form one variable grouping (Fig. 4). A second cluster groups specimens with relatively long muzzles, such as *Dinopithecus ingens*, *Theropithecus darti*, and *P. angusticeps*. This second cluster makes no distinction on the basis of size as *Pp. jonesi*, with a small, narrow, but relatively elongated snout, along with BF 43 (*Pp. whitei*), with its particularly tall but relatively truncated snout and short palate, are

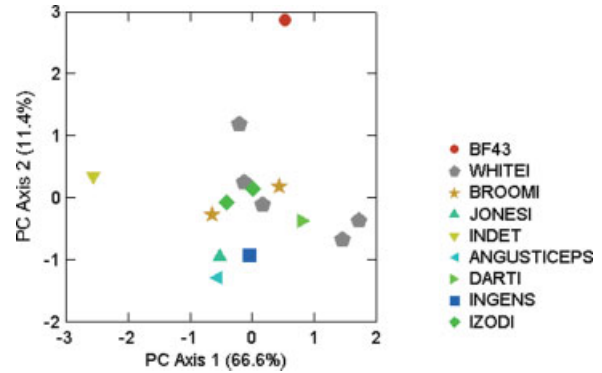


Fig. 5. Principal components analysis of fossil papionins. [Color figure can be viewed in the online issue, which is available at www.interscience.wiley.com.]

TABLE 6. PCA component loadings for eleven interlandmark distances

Trait	Interlandmark distance	PC Axis 1	PC Axis 2
1	1–4: Palatal length	0.884	–0.326
2	1–5: Anterior snout length	0.904	0.051
3	2–3: Premaxilla breadth	0.822	–0.031
4	6–7: Upper maxillary breadth	0.800	0.346
5	8–9: Lower maxillary breadth	0.683	0.354
6	12–13: Posterior alveolar breadth	0.741	0.297
7	14–15: Mid-alveolar breadth	0.786	–0.556
8	1–13: Alveolar length	0.940	–0.291
9	1–11: Premaxilla height	0.842	0.150
10	11–12: Snout length	0.889	–0.284
11	4–6: Snout height	0.676	0.563

grouped with the more derived papionin taxa (*Dinopithecus*, *Theropithecus*, *P. angusticeps*).

The morphological distance across specimens is considerable, suggesting that this sample represents a large degree of interindividual variability. Some of the closest distances between specimens are those clustering juvenile and adult pairs (MP 224 and MP 239; MP 166 and TP 9; SK 554 and MP 222) all of which represent different species. There are no relatively short morphological distances based solely on traditional taxonomic assessments.

Principal components analysis. A principal components analysis of eleven facial traits across fifteen specimens polarizes short and narrow snouts from larger prognathic ones on the first axis, and extremely tall, and broad maxilla from elongated and relatively narrow maxilla on principal components (PC) axis 2 (Fig. 5). PC axis 1, explaining two-thirds of the variance, polarizes the young juvenile indeterminate *Parapapio* specimen, MP 166, from the large male *Pp. whitei* adults, MP 221 and MP 223. PC 1 also separates *P. angusticeps*, *Pp. jonesi*, and a *Pp. broomi* juvenile (MP 224) with short and narrow snouts from the prognathic *Pp. whitei* adults from Makapansgat, and to some extent, from MP 222 (*Theropithecus darti*). The positive loadings for all of the traits suggest that this axis largely represents size differences (Table 6). PC axis 2, explaining 11% of the variance, separates *Pp. whitei* from Bolt's Farm, and to some extent, *Pp. whitei* from Taung, from *P. angusticeps*, *Pp. jonesi* and *Dinopithecus ingens*. BF 43, with its uniquely tall and posteriorly broadened snout is separated from other specimens. *P. angusticeps*, *Pp. jonesi*,

TABLE 7. Variance-covariance matrix of eleven interlandmark distances¹

	1	2	3	4	5	6	7	8	9	10	11
1	112.295										
2	38.6076	40.7412									
3	12.4218	10.2967	10.2505								
4	33.6771	30.0758	4.16606	45.2342							
5	90.5281	45.0311	5.1341	89.3755	319.465						
6	7.20341	7.45795	9.32902	9.20326	36.02	18.675					
7	33.5485	11.0438	6.73093	5.04698	16.3854	2.94314	17.7669				
8	79.532	34.7263	11.0627	33.8279	69.4372	5.65625	27.7672	67.8256			
9	12.5143	15.2489	5.55548	13.8018	18.8069	4.72775	4.40473	12.7116	8.76808		
10	70.1085	25.0783	7.03147	26.1613	46.3838	3.6529	20.8661	57.122	7.29817	55.985	
11	11.3889	16.5959	7.90612	20.4738	40.7642	17.2572	-6.37058	7.86546	6.57824	13.6439	40.2028

¹ Large variances and covariances are in bold. See Table 2 for definitions of these 11 interlandmark distances.

TABLE 8. Mahalanobis distances between 13 individuals¹

	BF43	KA194	MP221	MP222	MP223	MP239	SK554	STS254A	STS565	SWP12	TP10	TP11	TP9
BF43	0.0												
KA194	23.8	0.0											
MP221	18.2	19.3	0.0										
MP222	23.3	23.4	15.8	0.0									
MP223	22.3	22.3	12.2	23.7	0.0								
MP239	16.6	14.5	10.6	11.8	9.6	0.0							
SK554	23.6	23.2	15.0	23.5	23.1	15.8	0.0						
STS254A	22.0	22.5	23.0	20.1	17.5	15.2	19.9	0.0					
STS565	23.3	23.2	14.8	23.9	23.8	12.5	23.7	19.5	0.0				
SWP12	23.6	23.0	16.9	22.2	21.2	19.3	23.4	21.2	22.5	0.0			
TP10	20.6	21.9	22.3	20.3	18.0	7.7	18.6	22.7	19.4	18.5	0.0		
TP11	23.4	23.1	14.3	23.8	23.6	13.7	23.9	19.3	23.9	22.8	18.7	0.0	
TP9	22.4	23.3	19.0	23.1	22.0	8.6	21.6	21.5	22.6	20.5	22.9	22.0	0.0

¹ This analysis excluded one trait (lower maxillary breadth) and two juveniles (MP 166 and MP 224). Relatively short D^2 distances are in bold.

and *Dinopithecus ingens* are polarized from BF 43 by their relatively elongated snouts and broad mid-palates.

The component loadings suggest that all of the 11 variables are positively correlated with the first axis. A more detailed examination of the variation within traits, and the relationships between traits, reveals how patterns of correlation/covariance are influencing the structure of the data. A variance/covariance matrix shows that a number of interlandmark distances exhibit large covariances (palatal length, alveolar length, snout length; Traits 1, 8, and 10) suggesting that they may be measuring the same trait (Table 7). However, palatal length and alveolar length do differ in important ways. For example, SK 554 exhibits an elongated palate, but not a particularly long tooth row (Fig. 3c), and some individuals, such as BF 43, have tall, but not long snouts (PCA 2, Table 5). Palatal length, alveolar length, and snout length (Traits 1, 8, and 10) exhibit a large amount of ontogenetic variation (e.g., Fig. 3c). To focus on adult differences, MP 224 and MP 166 were removed before calculating Mahalanobis' distances between individual specimens but the *Dinopithecus* nonadult, SK 554, was retained to avoid instability in the V/CV matrix from a reduced number of individuals. Likewise, the extreme amount of variance on lower maxillary breadth (Table 7) stemming from the particularly narrow lower cheek widths characterizing *Pp. jonesi* (STS 565) and *P. angusticeps* (KA 194) (Fig. 3d) necessitated the removal of this trait prior to calculating D^2 distances.

Mahalanobis' distances. The fact that many Mahalanobis' distances are similar in magnitude, particularly with respect to MP 239 (*Pp. whitei*), reflects a distinct

lack of substructuring or subclustering (Table 8). MP 239 happens to exhibit values that fall in the middle of the distribution of most interlandmark distances. Some of the shortest D^2 distances are between specimens from Makapansgat, although not all individuals from this site exhibit reduced D^2 distances. The D^2 distances between *Pp. whitei* specimens (including BF 43) are similar, and generally greater than those between other individuals, at least in magnitude. The small D^2 distance between MP 221 and MP 223 is reflected in the positions of these two male *Pp. whitei* specimens in all of the bivariate comparisons. Importantly, differences in the magnitude between populations from which the individuals were derived, or other sampling-related issues, may have altered or inflated these distances (Ackermann, 2005). Although estimates of variance and covariance from extremely small samples sizes are suspect, and unequal numbers of individuals in each purported species increase unreliability (Ackermann, 2002, 2005), the lack of a clear taxonomic signal or site effect within these D^2 distances largely corroborate the analyses presented above.

DISCUSSION

Our analyses clearly indicate that there is substantial morphological variation among the fossil *Parapapio* specimens. Yet, despite some similarity among some *Pp. whitei* and *Pp. broomi* adults, this variation does not clearly align with traditional taxonomic designations, nor does it align with site location. Here, we will discuss two possible explanations for the patterns of variation seen among these specimens: 1) that the taxonomic

assignments as they currently stand are incorrect, and 2) that the variation is indicative of substantial time depth in our sample, and itself provides a biochronological signal. In particular, this would suggest substantial time depth in the Makapansgat and Sterkfontein cave deposits, from which the majority of our sample derives.

These analyses show some clear differences among genera, which indicates that the chosen aspects of morphology are (at least at this level) useful taxonomic indicators. For example, *Theropithecus darti* differs from the other specimens in its narrow premaxilla, which suggests a smaller more compact anterior dentition. Smaller incisors in this species may correspond to a particular dietary regimen or food processing behavior. Specimens attributed to *Parapapio* are generally distinct from other fossil papionins in bivariate comparisons. Similarly, although it was not possible to compare the ontogenetic trajectories across all species, there are important developmental differences among genera; this highlights the potential for reconstructing the facial evolution of Pliocene southern African papionins. *Pp. broomi* may be the best sample to model ontogenetic shifts among Pliocene cercopithecids of southern Africa (Williams et al., 2005). It is probably represented by the greatest number of juveniles, including (perhaps) the juvenile *Parapapio* species-indeterminate Makapansgat and Sterkfontein material. It is also possible to examine ontogenetic patterns of *Dinopithecus ingens*. When compared with a fragmentary adult, the well preserved juvenile, SK 554, shows that elongation of the palate in this species occurred early in postnatal ontogeny. Furthermore, the adult *Dinopithecus* palate of SK 553 is particularly elongated when compared with *Parapapio* adults (Fig. 3a), demonstrating the evolution of extreme prognathism (and probably pronounced sexual dimorphism) of Pleistocene male papionins.

But while higher level taxonomic categories are often consistent with differences in morphology in these analyses, they are not uniformly consistent. Similarly, species-level distinctions are often not upheld, making it difficult to interpret the biochronological signal at this level. For example, although specimens attributed to *Parapapio* are generally distinct from other fossil papionins in bivariate comparisons, as mentioned above, multivariate treatments of the data tend to link smaller forms from separate genera (e.g., *Parapapio* and *P. izodi*) together. In fact, the larger, more derived specimens differ from one another as much as they do from the smaller fossil papionins. Such differences in size may indicate temporal relationships, as revealed in the growth of Pliocene *Parapapio* and Pleistocene *Dinopithecus*. However, in the cluster analysis, *Pp. jonesi*, a small papionin, is divergent from *Parapapio* and *P. izodi*, indicating that size is only one of many traits that tend to separate individuals. For several facial dimensions, *P. izodi*, and to a lesser extent, *P. angusticeps*, represented here by KA 194 from Kromdraai, may resemble fossil *Parapapio*, more than they do modern *Papio*. The fact that most of the *P. angusticeps* and *P. izodi* specimens we examined are female may, in part, explain their resemblance to *Parapapio*.

Even within the genus *Parapapio* the pattern is complex. Although for many interlandmark distances *Pp. whitei*, *Pp. broomi*, and in some instances *Pp. jonesi*, can be considered scaled versions of one another (see also Fourie, 2006), *Parapapio* is hardly a monotypic group. In particular, two *Parapapio* specimens differ substantially:

STS 565 and BF 43. The single *Pp. whitei* specimen from Bolt's Farm, BF 43, differs from all other *Parapapio* specimens, and indeed, all other cercopithecoid fossils examined in this study. This specimen was originally attributed to *Pp. whitei* by Freedman (1965), and later referred to *Pp. broomi* by Maier (1970). Subsequent dental metric results corroborated a *Pp. whitei* attribution (Freedman and Stenhouse, 1972). Although some Taung *Parapapio* have been compared with BF 43 in earlier analyses (Freedman, 1965), in our cluster and principal components analyses, BF 43 is distinct. Mahalanobis' distances for BF 43 were most similar to some *Pp. whitei* from Makapan (MP 239, MP 221) and one *P. izodi* specimen from Taung (TP 10), but not particularly so with respect to the distances between other individuals. What differentiates BF 43 is a particularly tall and expanded muzzle. Meanwhile, *Pp. jonesi*, represented here by STS 565, is distinct in some facial dimensions from all other individuals ascribed to *Parapapio*, being most similar to *P. izodi* and *P. angusticeps*.

While taxonomic inconsistencies may explain some of the diversity within taxa, much of the variation probably reflects vast temporal differences among the fossils, providing an important biochronological signal. This is particularly interesting with respect to the morphologically distinctive BF 43, as the biostratigraphic dating of this specimen is hampered by the difficulty in reconstructing the original pit positions of the 1947–48 excavations (Sénégal et al., 2002). The Bolt's Farm site has yielded at least three well-preserved crania from three different taxa: *Pp. whitei* (BF 43), *Cercopithecoides williamsi* (BF 42A), and *P. h. robinsoni* (BF 38), as well as fragmentary material from Pit 6 attributed to *P. h. robinsoni* (Williams, unpublished data from the University of California, Berkeley collection). The diversity of this site indicates a complex depositional history that spans several time periods. While BF 43 and BF 42A derive from Pit 23, BF 38 was recovered from Pit 6 (Freedman, 1965; Williams, unpublished data from original fossil catalogues, School of Anatomical Sciences, University of the Witwatersrand). Since *P. h. robinsoni* is also found at Kromdraai and Swartkrans, two Pleistocene sites, and *Cercopithecoides williamsi* is found primarily at the older sites of Sterkfontein Member 4, Makapansgat and Taung (and presumably at Haasgat, Kromdraai B and Swartkrans Member 2), BF 43 may derive from late Pliocene sediments and could represent the terminal aspects of the larger *Parapapio* radiation that took place before widespread climate deterioration and oscillation occurred in the early Pleistocene. Bolt's Farm Pit 6 was probably deposited during Delson's (1984, 1988) A-C zone 5 or later (Table 1).

The possibility that the smallest species of *Parapapio* survived these climatic events is evidenced by the remains of numerous fragmentary facial remains of *Pp. jonesi*, particularly from Swartkrans Members 1 and 2 (Brain, 1981; Watson, 2004). Our *Pp. jonesi* sample, consisting of STS 565, arguably the most complete representative of this species (cf. Maier, 1970), showed similarities to *Papio* species in some aspects of facial morphology. The degree to which *Parapapio* survived the Pliocene-Pleistocene transition is contingent on whether the specimens referred to *Pp. jonesi* from Sterkfontein and Makapansgat (Freedman and Stenhouse, 1972) represent the same taxon discovered at Kromdraai and Swartkrans (cf. Delson, 1984; McKee et al. 1995; Jablonski, 2002). The fact that *Pp. jonesi* is represented at

Sterkfontein could suggest that this site spans the Plio-Pleistocene boundary. The diversity of fossil cercopithecids at Makapansgat, including *Theropithecus darti*, may suggest that, like Sterkfontein, the depositional history of Makapansgat may also have extended from the middle Pliocene into the early Pleistocene. Although *Theropithecus darti* is arguably the most derived fossil papionin in our sample (Jablonski, 2002), it is smaller and exhibits less extreme craniodental features compared with *Theropithecus oswaldi danieli* (Szalay and Delson, 1979) from Swartkrans Member 1–3 (Watson, 2004).

Although we cannot address the general degree to which morphometric data can reproduce assessments made using alpha taxonomy, we can say that our data tend to group *Pp. broomi* and *Pp. whitei* across sites as distinct from other fossil papionins, and that the largest males are often attributed to *Pp. whitei*, while smaller males, females, subadults, and juveniles are overwhelmingly referred to *Pp. broomi*. It is entirely possible that all of these specimens (from A-C zones 3 and 4, Table 1) belong to a single variable taxon (*Parapapio broomi* sensu Jones (1937)), and should be differentiated only on a subspecific level. *Pp. whitei* could then be reserved for the enigmatic Bolt's Farm Pit 23 specimen, BF 43, while the distinctive STS 565 fossil should continue to be referred to *Pp. jonesi*. Taxonomic revisions aside, the tremendous morphological variation across these fossil papionins, particularly as revealed in the Mahalanobis' distances and the lengths of the branches in the cluster analysis, suggests a considerable time depth to these karstic deposits.

The biochronological implications formed on the basis of these morphological discontinuities suggest that *Australopithecus* from Sterkfontein, Makapansgat, and Taung could have been deposited in the Pliocene or close to the Plio-Pleistocene boundary, or in the earliest part of the Pleistocene, depending on the location of the fossils within each cave. Judging from the general replacement of smaller papionins with larger, more prognathic and highly derived forms, the robust australopithecines at Swartkrans and Kromdraai were securely deposited within the last two million years, primarily in the Pleistocene.

CONCLUSIONS

There is a tremendous amount of morphological diversity among Plio-Pleistocene papionins in South Africa. The fact that this diversity does not always clearly align with species categories suggests that these boundaries, or at least the placement of certain fossils, need to be reconsidered. It is also possible that some of the variation reflects a biochronological signal, as calibrated by geochronological ordination of morphological discontinuities. For instance, in spite of the diversity of taxa at Taung, this site does not preserve any large, dimorphic papionins, indicating that it originates from Pliocene deposits, whereas Swartkrans and Kromdraai, with a greater number of prognathic and highly derived forms (*Dinopithecus*, *Theropithecus* and *Papio*), and fewer smaller forms—represented exclusively by *Pp. jonesi*—are clearly Pleistocene sites. Makapansgat, Sterkfontein, and Bolt's Farm perhaps span long intervals of time, from middle to late Pliocene to early Pleistocene. Both Makapansgat and Sterkfontein preserve a wealth of *Parapapio* taxa, and although *Theropithecus darti* stems

from Makapansgat, and *Pp. jonesi* derives from Sterkfontein, these forms are scarce and not as divergent as clearly related forms from the later Pleistocene sites. The implications drawn from these observations help to situate the *Australopithecus* remains found in the same depositional contexts as these fossil papionins.

ACKNOWLEDGMENTS

F. Thackeray (Transvaal Museum, NFI) kindly granted access to materials in his care. P.V. Tobias and L. Berger generously allowed S.R.L. access to materials from the School of Anatomical Sciences, University of the Witwatersrand. J. McKee offered valuable advice in the early stages of the project. The kind assistance of K. Kuykendall, F. Thackeray, and S. Potze to R.R.A. and F.L.W. is gratefully acknowledged.

LITERATURE CITED

- Ackermann RR. 2002. Patterns of covariation in the hominoid craniofacial skeleton: Implications for paleoanthropological models. *J Hum Evol* 43:167–187.
- Ackermann RR. 2005. Variation in Neanderthals: A response to Harvati (2003). *J Hum Evol* 48:643–646.
- Benefit BR. 1999. Biogeography, dietary specialization and the diversification of African Plio-Pleistocene monkeys. In: Bromage TG, Schrenk F, editors. African biogeography, climate change, and human evolution. Oxford: Oxford University Press. p 172–188.
- Berger LR, Keyser AW, Tobias PV. 1993. Gladysvale: First early hominid site discovered in South Africa since 1948. *Am J Phys Anthropol* 92:107–111.
- Brain CK. 1981. The hunters or the hunted? An introduction to African cave taphonomy. Chicago: University of Chicago Press.
- Broom R, Jensen JS. 1946. A new fossil baboon from the caves at Potgietersrust. *Ann Transvaal Museum* 20:337–340.
- Delson E. 1984. Cercopithecoid biochronology of the African Plio-Pleistocene: Correlations among eastern and southern hominid-bearing localities. *Cour Forsch-Inst Seneckenberg* 69:199–218.
- Delson E. 1988. Chronology of South African Australopithecoid site units. In: Grine FE, editor. Evolutionary history of the robust australopithecines. New York: Aldine. p 317–324.
- Delson E. 1992. Evolution of old world monkeys. In: Jones JS, Martin RD, Pilbeam D, Bunney S, editors. The Cambridge encyclopedia of human evolution. Cambridge: Cambridge University Press. p 217–222.
- Eisenhart WL. 1974. The fossil cercopithecoids of Makapansgat and Sterkfontein. BA Thesis (unpublished), Harvard University, Cambridge, MA.
- El-Zaatari S, Grine FE, Teaford MF, Smith HF. 2005. Molar microwear and dietary reconstructions of fossil Cercopithecoida from the Plio-Pleistocene deposits of South Africa. *J Hum Evol* 49:180–205.
- Fourie NH. 2006. Dietary ecology and niche separation among three closely related species (*Parapapio jonesi*, *Pp. whitei* and *Pp. broomi*) of South African Plio-Pleistocene Cercopithecoida from Makapansgat Limeworks site. MS Thesis (unpublished), University of Cape Town.
- Freedman L. 1957. The fossil cercopithecoida of South Africa. *Ann Transvaal Museum* 23:122–262.
- Freedman L. 1960. Some new fossil cercopithecoid specimens from Makapansgat, South Africa. *Palaeontol Afr* 7:7–45.
- Freedman L. 1961. New cercopithecoid fossils, including a new species, from Taung, Cape Province, South Africa. *Ann S Afr Museum* 46:1–14.
- Freedman L. 1965. Fossil and subfossil primates from the limestone deposits at Taung, Bolt's Farm and Witkrans, South Africa. *Palaeontol Afr* 9:19–48.

- Freedman L. 1976. South African fossil Cercopithecoidea: A reassessment including a description of new material from Makapansgat, Sterkfontein and Taung. *J Hum Evol* 5:297–315.
- Freedman L, Brain CK. 1972. Fossil cercopithecoid remains from the Kromdraai australopithecine site (Mammalia: Primates). *Ann Transvaal Museum* 28:1–16.
- Freedman L, Stenhouse NS. 1972. The *Parapapio* specimens of Sterkfontein, Transvaal, South Africa. *Palaeontol Afr* 14:93–111.
- Frost SR, Marcus LF, Bookstein FL, Reddy DP, Delson E. 2003. Cranial allometry, phylogeography, and systematics of large-bodied papionins (Primates: Cercopithecinae) inferred from geometric analysis of landmark data. *Anat Rec* 275:1048–1072.
- Gear JHS. 1926. A preliminary account of the baboon remains from Taungs. *S Afr J Sci* 23:731–747.
- Jablonski NG. 2002. Fossil Old World monkeys: The late Neogene radiation. In: Harwig, WC, editor. *The primate fossil record*. Cambridge: Cambridge University Press. p 225–300.
- Jones TR. 1937. A new fossil primate from Sterkfontein, Krugersdorp, Transvaal. *S Afr J Sci* 33:709–728.
- Keyser AW, Menter CG, Moggi-Cecchi J, Pickering TR, Berger LR. 2000. Drimolen: A new hominid-bearing site in Gauteng, South Africa. *S Afr J Sci* 96:193–197.
- Leigh SR. 2006. Cranial ontogeny of *Papio* baboons (*Papio hamadryas*). *Am J Phys Anthropol* 130:71–84.
- Leigh SR, Shah NF, Buchanan LS. 2003. Ontogeny and phylogeny in papionin primates. *J Hum Evol* 45:285–316.
- Maier W. 1970. New fossil Cercopithecoidea from the lower Pleistocene cave deposits of the Makapansgat limeworks, South Africa. *Palaeontol Afr* 13:69–107.
- McKee JK. 1993a. Faunal dating of the Taung fossil hominid site. *J Hum Evol* 25:363–376.
- McKee JK. 1993b. Taxonomic and evolutionary affinities of *Papio izodi* fossils from Taung and Sterkfontein. *Palaeontol Afr* 30:43–49.
- McKee JK, Keyser AW. 1994. Craniodental remains of *Papio angusticeps* from the Haasgat cave site, South Africa. *Int J Primatol* 15:823–841.
- McKee JK, Thackeray JF, Berger LR. 1995. Faunal assemblage seriation of southern African Pliocene and Pleistocene fossil deposits. *Am J Phys Anthropol* 96:235–250.
- Partridge TC. 2000. Hominid-bearing cave and tufa deposits. In: Partridge TC, Maud RR, editors. *The Cenozoic of southern Africa*. New York: Oxford University Press. p 100–129.
- Partridge TC, Shaw J, Heslop D. 2000. Note on recent magnetostratigraphic analyses in Member 2 of the Sterkfontein formation. In: Partridge TC, Maud RR, editors. *The Cenozoic of southern Africa*. New York: Oxford University Press. p 129–130.
- Sénégal F, Thackeray JF, Gommery D, Braga J. 2002. Palaeontological sites on 'Bolt's Farm', Sterkfontein Valley, South Africa. *Ann Transvaal Museum* 39:65–67.
- Szalay FS, Delson E. 1979. *Evolutionary history of the primates*. New York: Academic Press.
- Thackeray JF, Kirschvink JL, Raub TD. 2002. Palaeomagnetic analyses of calcified deposits from the Plio-Pleistocene hominid site of Kromdraai. *S Afr J Sci* 98:537–539.
- Vrba ES. 1996. Habitat theory in relation to the evolution in African Neogene biota and hominids. In: Bromage TG, and Schrenk F, editors. *African biogeography, climate change, & human evolution*. New York: Oxford University Press. p 19–46.
- Vrba ES. 2000. Major features of Neogene mammalian evolution in Africa. In: Partridge TC, Maud RR, editors. *The Cenozoic of southern Africa*. New York: Oxford University Press. p 277–304.
- Watson V. 2004. Composition of Swartkrans bone accumulation, in terms of skeletal parts and animals represented. In: Brain CK, editor. *Swartkrans: A cave's chronicle of early man*, 2nd ed. Transvaal Museum monograph No. 8. Pretoria: Transvaal Museum. p 35–74.
- Williams FL. 2004. Testing for hyperpaedomorphosis in southern African Plio-Pleistocene baboons. *Am J Phys Anthropol* 36 (Suppl):208, 209.
- Williams FL, Ackermann RR, Leigh SR. 2005. Craniofacial growth and development in *Parapapio* and other Plio-Pleistocene southern African cercopithecines. *Am J Phys Anthropol Suppl* 37:223.